

Western Kentucky University

TopSCHOLAR®

Masters Theses & Specialist Projects

Graduate School


Fall 2020

Developing Novel TALE-Based Rapid Detection of Pathogenic DNA Utilizing 2D Graphene Oxide Nanosheets and Quantum Dots

Narayan Neupane

Western Kentucky University, narayanneupane35@gmail.com

Follow this and additional works at: <https://digitalcommons.wku.edu/theses>

 Part of the [Analytical Chemistry Commons](#), and the [Biochemistry, Biophysics, and Structural Biology Commons](#)

Recommended Citation

Neupane, Narayan, "Developing Novel TALE-Based Rapid Detection of Pathogenic DNA Utilizing 2D Graphene Oxide Nanosheets and Quantum Dots" (2020). *Masters Theses & Specialist Projects*. Paper 3473.

<https://digitalcommons.wku.edu/theses/3473>

This Thesis is brought to you for free and open access by TopSCHOLAR®. It has been accepted for inclusion in Masters Theses & Specialist Projects by an authorized administrator of TopSCHOLAR®. For more information, please contact topscholar@wku.edu.

DEVELOPING NOVEL TALE-BASED RAPID DETECTION OF PATHOGENIC
DNA UTILIZING 2D GRAPHENE OXIDE NANOSHEETS AND QUANTUM DOTS

A Thesis
Presented to
The Faculty of the Department of Chemistry
Western Kentucky University
Bowling Green, Kentucky

In Partial Fulfillment
Of the Requirements for the Degree
Master of Science

By
Narayan Neupane

December 2020

DEVELOPING NOVEL TALE-BASED RAPID DETECTION OF PATHOGENIC
DNA UTILIZING 2D GRAPHENE OXIDE NANOSHEETS AND QUANTUM DOTS

Date Recommended 11/19/2020

Moon-Soo Kim Digitally signed by Moon-Soo Kim
Date: 2020.11.20 12:58:13 +09'00'

Dr. Moon-Soo Kim, Director of Thesis

Kevin Williams Digitally signed by Kevin Williams
Date: 2020.11.19 15:47:14 -06'00'

Dr. Kevin Williams

Matthew Nee Digitally signed by Matthew Nee
Date: 2020.11.19 18:09:45 -06'00'

Dr. Matthew Nee



Associate Provost for Research and Graduate Education

I dedicate my thesis to my parents, Huma Kanta Neupane and Deu Kumari Neupane for allowing me to gain the best possible education as well as to my siblings, Durga Prasad Neupane and Ambika Kandel for their continuous support and faith in me.

ACKNOWLEDGMENTS

First and foremost, I would like to express my deepest gratitude and sincere thanks to Associate Professor Dr. Moon-Soo Kim, my research advisor for accepting me to work as a graduate student in her laboratory. Through her immense support and continuous guidance, I was able to gain significant research skills and experiences. Her motivation to hard work and to pro-actively think will always encourage me to work more as a scientific researcher in the future. She not only provided me a full financial support as an RA, but also provided full research materials to run my thesis project. I would hardly imagine a better mentor than her.

My sincere thanks also go to Professor and Department Chair Dr. Kevin Williams and Professor Dr. Matthew Nee, members of my thesis committee for their valuable time and constructive feedbacks on my thesis as well as my research.

I am also thankful to my lab mates Jiyoun Shim, Van Thuan Nguyen, Dat Thinh Ha, Joel Omage, Colleen Jackson, Kayser Rebekah, Wendy Cecil and Kenneth Schlabach for their continuous cooperation in the lab.

I would also like to thank our former department chair Professor Dr. Stuart Burris and Professor Dr. Eric Conte for accepting me as a graduate student with full assistantship throughout my degree. I would also appreciate the Office Associate, Ms. Haley Smith for assisting me in all kinds of paperwork and also patiently answering my questions as well as replying my emails.

TABLE OF CONTENTS

CHAPTER I - INTRODUCTION.....	1
1. DNA Detection and Recognition Methods.....	1
2. Transcriptional Activator-like Effectors (TALEs).....	2
3. Applications of TALEs.....	4
3.1 TALE Nucleases (TALENs).....	4
3.2 TALE Recombinases (TALERS).....	5
3.3 TALE Artificial Transcription Factors (TALE-ATFs).....	5
4. Pathogen Detection.....	6
5. Detection Methods.....	6
5.1 Detection based on Fluorescence Resonance Energy Transfer.....	6
5.2 Quantum dots in diagnostic applications.....	7
5.3 Graphene oxides as biosensors.....	9
6. Aims of study.....	9
CHAPTER II – EXPERIMENTAL.....	12
1. Engineering of TALEs.....	12
2. Expression and Purification of TALEs.....	12
3. Preparation of GO.....	14
4. Quantum dot labeling.....	14
5. Graphene oxide quenching.....	16
6. TALE-GO assay.....	17
CHAPTER III – RESULTS AND DISCUSSION.....	18

1. Expression and purification of TALEs.....	18
2. Characterization of GO.....	20
3. Quantum dot labeling of TALEs.....	24
4. GO Quenching Efficiency.....	24
5. Sensitivity.....	29
CHAPTER IV – CONCLUSION.....	31
BIBLIOGRAPHY.....	33

LIST OF FIGURES

Figure 1. A schematic of a TAL effector showing the N-terminus, central repeat and C-terminus regions.....	3
Figure 2. Structure of a single TAL effector highlighting the RVDs at position 12 and 13 of the repeat.....	4
Figure 3. Jablonski diagram illustrating FRET phenomenon and showing energy states for both donor and acceptor molecules.....	7
Figure 4. Structure of a monolayer graphene oxide showing various oxygen containing functional groups.....	9
Figure 5. A schematic diagram showing GO-FRET based assay using QD-labeled TALEs for detecting dsDNA.....	11
Figure 6. EDC/NHS bioconjugation chemistry showing the formation of a stable peptide bond.....	16
Figure 7. SDS-PAGE gel of TALE stx2 236 from <i>E. coli</i> BL-21 expression and purification.....	19
Figure 8. TEM image of monolayer GO sheets.....	21
Figure 9. TEM image of QD-labeled stx2 236 TALEs on GO surface.....	21
Figure 10. AFM image of bare GO surface and the height profile of corresponding yellow lines.....	22
Figure 11. AFM image of QD-labeled stx2 236 TALEs on GO surface and the height profile of corresponding yellow line.....	23
Figure 12. GO Quenching efficiency from 5 to 70 $\mu\text{g/mL}$	27

Figure 13. GO Quenching efficiency from 2 to 10 $\mu\text{g/mL}$	29
Figure 14. The limit of detection of TALE stx2 236.....	30

LIST OF TABLES

Table 1. Design of novel TALE stx2 236 RVD sequence to target Shiga Toxin gene at two adjacent locations.....	12
---	----

DEVELOPING NOVEL TALE-BASED RAPID DETECTION OF PATHOGENIC DNA UTILIZING 2D GRAPHENE OXIDE NANOSHEETS AND QUANTUM DOTS

Narayan Neupane

December 2020

40 pages

Directed by: Dr. Moon-Soo Kim, Dr. Kevin Williams and Dr. Matthew Nee

Department of Chemistry

Western Kentucky University

A faster method of quantitative detection of specific dsDNA of pathogenic bacteria such as the Shiga toxin 2 gene (*stx2*) present in *E. coli* O157:H7 is of great importance. There is a need for a simple and facile method for sensitive detection of pathogenic gene which is crucial for the prevention and earlier treatment of any infectious diseases. A Transcriptional Activator-Like Effector (TALE) is a novel class of DNA-binding proteins with the unique modularity, flexibility and easy programmability compared to previously discovered DNA-binding proteins. TALEs can bind to any DNA sequences through its unique variable di-residues (RVDs) present in each repeat in the DNA-binding region of the protein. Graphene oxide (GO) is a 2D-nanosheet formed by the oxidation of graphite. It has many oxygen-containing functional groups such as carboxyl, hydroxyl, carbonyl and epoxide in its structure, allowing for interaction with biomolecules such as DNA and proteins. The GO has gained wide popularity because of its unique properties such as larger surface area, high water dispersibility and excellent biocompatibility. Quantum dots (QDs) are metallic, semi-conducting nanoparticles possessing unique electrical, physical and optical properties.

Our goal was to develop a rapid method to quantitatively detect pathogenic double stranded (ds) DNA in the *stx2* gene encoding the Shiga toxin present in *E. coli* O157:H7.

Novel TALEs were designed to detect the *stx2* gene and were cloned into the pMAL c2x vector system replacing AvrBs3 TALE protein for bacterial BL-21 *E. Coli* expression. The TALE proteins were purified by His-tag affinity chromatography using Ni-resin. TALE proteins were then labeled with CdSe/ZnS QDs using EDC/NHS bioconjugation to create a stable peptide bond between the QDs and the proteins. Labeling efficiency was higher, > 90% compared to the previously discovered Zinc Finger Proteins (ZFPs). The GO quenching assay was performed to determine the optimal concentration of GO that quenches QD signals via fluorescent resonance energy transfer (FRET). The optimal sensitivity conditions were determined to be 20 nM of QD-labeled proteins and 3 µg/mL of GO. The GO assay took in less than 30 minutes in a simple laboratory setting. The limit of detection of TALE *stx2* 236 was determined to be 200 pM which is equivalent to 40 fmol of the target oligonucleotide. In summary, we have demonstrated the novel application of a new class of DNA binding protein TALEs and 2D nanosheet GO as a sensing platform for detecting pathogen-specific dsDNA in a simple assay.

CHAPTER I. INTRODUCTION

1. DNA Detection and Recognition Methods

There is a growing need for sequence specific and sensitive detection of DNA for variety of applications such as disease diagnosis, pathogen detection, food safety and environment monitoring.¹ Numerous methods have been developed for DNA detection. However, the development of a simple, facile and sensitive detection technology for the detection of pathogen-specific double-stranded (ds) DNA is still challenging.

A number of current methods for pathogen detection and disease diagnostics involve DNA denaturation and subsequent hybridization with its complementary probes. Among these methods are polymerase chain reaction (PCR), DNA microarray and fluorescence in-situ hybridization (FISH).^{2,3,4} PCR requires multiple primers and precise thermal cycling conditions for nucleic acid amplification even though it is faster and provides sensitive detection compared to traditional culture-based methods.⁵ DNA microarray is another commonly available technique which enable one to detect multiple pathogens simultaneously.⁶ The DNA microarrays may be disadvantageous because of requiring DNA labeling and hybridization with their complementary probes which could ultimately increase inaccuracy of the technique due to the cross-reaction of several probes with incorrect targets.⁷ FISH is another widely used technique for visual detection of specific DNA/RNA sequences but, it can be time-consuming with limited sensitivity as well as its standard protocol is not widely available.⁸ Thus, the shortcomings of these commonly available methods can be avoided through the direct and sensitive detection of specific dsDNA with the aid of DNA-binding proteins. DNA-binding proteins can allow simple,

fast and specific detection of pathogenic DNA sequences and avoid the need of laborious steps in denaturation and subsequent hybridization of dsDNA.^{9,10} This is the novel aspect of our study which would allow us to design a lab-on-a-chip technique for simple and facile DNA detection.

2. Transcriptional Activator-like Effectors (TALEs)

TALE is the largest effector family for the transcriptional activation of plant genes.¹¹ TALEs are novel class of DNA-binding proteins expressed and released by a plant pathogenic bacteria of genus *Xanthomonas* and released to infect a variety of plant hosts with the major host being rice plants.¹² Similar to Zinc Finger Proteins (ZFPs), TALE proteins can bind to the major grooves of dsDNA in a sequence-specific manner.¹³ However, they are completely unique in their structures, the mechanism of nucleotide binding specificity and the number of nucleotide targets compared to ZFPs.¹⁴ Through the investigation of the AvrBs3 family of TALE proteins, much of the information concerning the structure and function of TALE has been acquired.¹⁵ Figure 1 is a schematic diagram of a TAL effector showing an N-terminus flanking region, a C-terminus flanking region and a central DNA-binding region.¹⁶ The central DNA-binding region consists of a tandem repeat of 34 amino acids, allowing it to bind to the specific promoter region on DNA.¹⁷ Amino acid residues at number 12 and 13 of the repeats collectively named repeat variable di-residues (RVDs) determine the nucleotide to which the particular repeat binds.¹⁸ A single TAL effector in figure 2 highlights the amino acid residues, Histidine (H) and Aspartate (D), respectively at positions 12 and 13. These are collectively called RVDs. Each RVD recognizes single base and different RVDs have variable affinity for different

nucleotides.¹⁹ All TALE proteins require a 5' thiamine independently of other RVDs before the protein can bind to the DNA.²⁰ (Fig. 1) The RVDs bind sequentially in 5' end to 3' end direction once the first nucleotide is identified.²¹ Asparagine-Isoleucine (NI), Asparagine-Glycine (NG), Asparagine -Asparagine (NN) and Histidine-Aspartate (HD) are the commonly used RVDs in engineered proteins to bind adenine, thiamine, guanine and cytosine bases respectively.²²

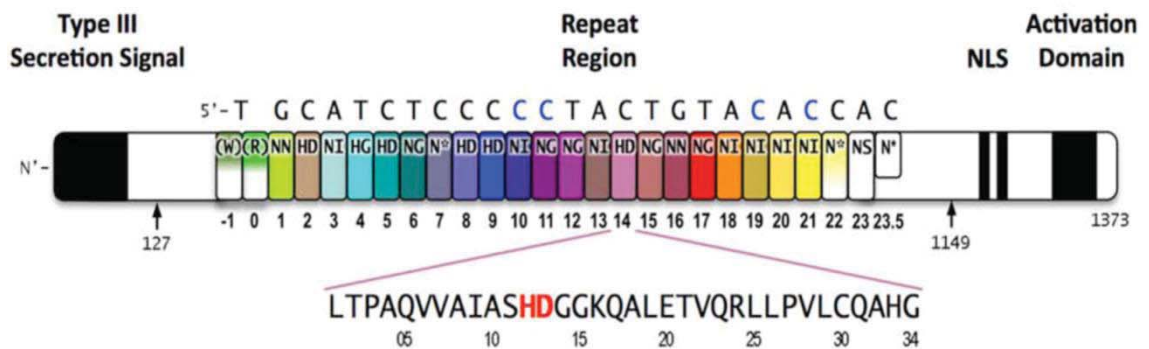


Figure 1. A schematic of a TAL effector showing N-terminus, central repeat and C-terminus regions (Mak et al, 2013)

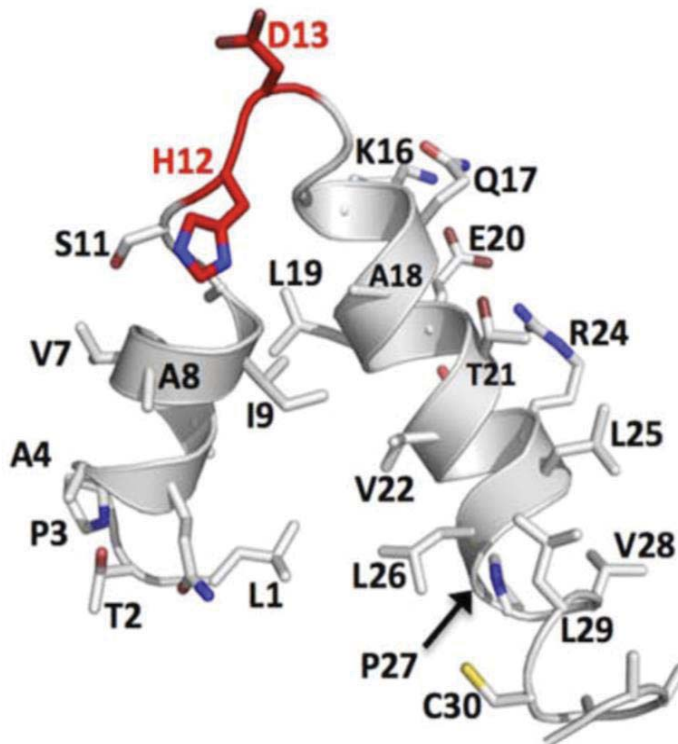


Figure 2. Structure of a single TAL effector highlighting the RVDs at position 12 and 13 of the repeat (Mak et. al, 2013)

3. Applications of TALEs

3.1 TALE Nucleases (TALENs)

TALENs are formed by the fusion of TALE with FokI nuclease domains and are responsible for the DNA double-stranded break (DSB).¹¹ These FokI nuclease domains are located at the C-terminus end of each TALE on either side.¹¹ TALENs are designed in pairs with a spacer in between so that the FokI nuclease domains have enough space to dimerize and cause a DNA DSB.²³ TALENs can be used as site-specific endonucleases for selective genomic cleavage.²³ The TALEN-based DSB is responsible for efficient targeted alteration of endogenous genes in plants, yeast, human somatic cells, and so on.^{24,25,26} AvrXa10 is a

TALE protein which has been used to design TALEN by manipulating the N- and C-terminal extensions on either side of the repeat domain.²⁷ Such TALENs have been optimized and show efficient cleavage of the target DNA in the human β -globulin gene with either little or no cytotoxicity.²⁷ In addition to this, TALENs have been used in the manipulation of the nucleotide sequence of protein dystrophin in Duchenne Muscular Dystrophy disease.²⁸ Moreover, TALENs have also been used in HIV1 gene therapy where there is about 45% of the disruption of genes.²⁶ Although similar level of gene disruption was achieved using ZFNs, TALENs-mediated gene disruption shows much lower cytotoxicity with reduced off-target cleavage.¹¹

3.2 TALE Recombinases (TALERS)

Because of the high specificity, single-stranded recombinases (SSR) have been used in genome engineering for the manipulation of DNA.¹¹ The target specificity of SSR can be altered by replacing the DNA-binding domain (DBD) of SSRs by novel DNA-binding TALEs.¹¹ TALEs ensure the specificity for inducing DSB and the recombinase assures the homology directed insertion of exogenous DNA.¹¹ By the use of TALER, the recombination of any DNA sequences in bacteria and mammalian cells is possible and the limitation of the modular targeting capacity of ZFRs can be minimized.¹¹

3.3 TALE Artificial Transcription Factors (TALE-ATFs)

Engineered TALEs can be fused to gene-specific activator and repressor domains to form TALE-ATFs.²⁹ TALEs fused with a VP64 domain have been shown to target a wide spectrum of DNA sequences at a similar or greater extent than ZFPs fused to VP64

domain.²⁹ Most TALE activators bearing a VP64 domain significantly induced expression of the *VEGF-A* gene in a wide range from 5.3 to 114-fold.²⁹

4. Pathogen Detection

The rise in antibiotic resistant pathogens has created a need for improvements in the rapid and specific detection of known the DNA sequences.³⁰ *E. coli* O157:H7 is a common food-borne pathogen producing pathogenic Shiga toxin (*stx2*) gene.³¹ The Center for Disease Control and Prevention (CDC) estimated in 2011 that 3,600 individuals were hospitalized because of the food-borne illness caused by the pathogen. The Shiga toxin causes severe gastrointestinal and urinary distress in humans and can sometimes lead to kidney failure or death.³² To control the spread and infection of harmful pathogens, many new antibiotics and novel diagnostic techniques are being developed.³³ A simple, quick and sensitive detection of pathogenic DNA is always critical for the early treatment of infectious diseases.

5. Detection methods

DNA diagnostics require a detection method with a signal transducer. Several non-PCR methods for DNA diagnostics have been developed as a sensitive method.³⁴

5.1 Detection based on Fluorescence Resonance Energy Transfer

Fluorescence resonance energy transfer (FRET) is a physical phenomenon in which there is distance-dependent transfer of energy from a donor molecule to an acceptor molecule.³⁵ Figure 3 is a Jablonski Diagram explaining the effect of FRET. Here, the energy that is released from the relaxation of the donor is taken up by a suitable acceptor

in close proximity, leading to the excitation of one of its electrons, and further to the emission of a photon by the acceptor. Since FRET is highly sensitive to distance between the molecules, different FRET-based biosensors composed of fluorophores and quenchers have been used to study various biochemical activities which produce changes in molecular proximity such as protein-protein interactions and enzyme activities.³⁶ FRET allows the visualization of these events through the use of various microscopic methods.³⁷ The donor molecules are called as fluorophores in which the energy absorbed by the donor is transferred to the acceptor.³⁸

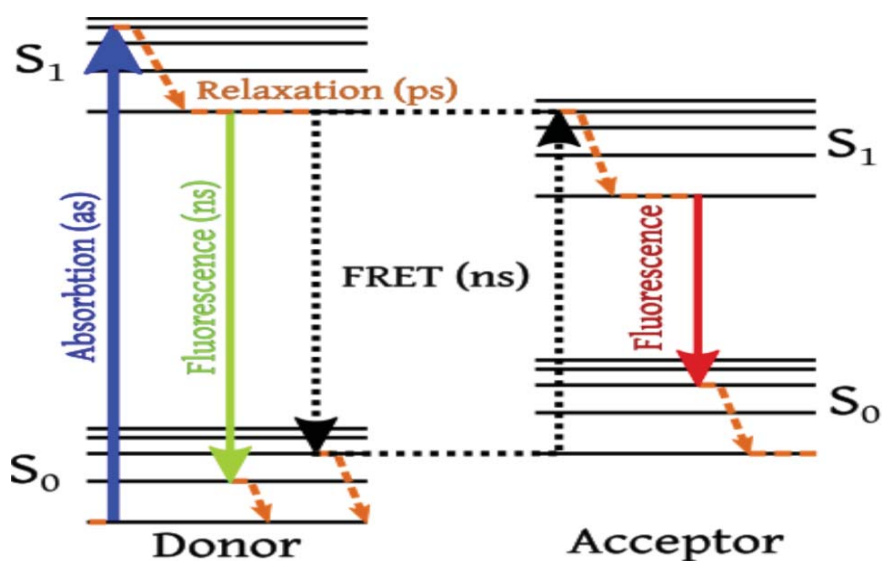


Figure 3. Jablonski diagram illustrating FRET phenomenon showing energy states for both donor and acceptor molecules

5.2 Quantum dots in diagnostic applications

Quantum dots (QDs) are metallic, semiconducting nanoparticles having unique optical, physical and electrical properties.³⁹ They can fluoresce at monochromatic

wavelengths after excitation by a single shorter wavelength, depending on the size and composition of the nanoparticle.⁴⁰ There is a considerable difference in their exciton discrete spectrum from a bulk crystal spectrum of the same chemical. This difference results in the change in the optical properties of the QDs compared to the bulk material.⁴¹ The QDs have the unique and exciting properties such as high quantum yield, size-tunable light emission and good chemical and photo-stability.³⁹ The QD consists of a core and a shell where a core is made up of materials such as cadmium-selenium (CdSe), cadmium-tellurium (CdTe), indium-phosphate (InP) or indium-arsenate (InAs).⁴² The shell is made up of zinc sulphide (ZnS) which stabilizes the core.⁴² Due to the broad absorption spectra, QDs can be excited by a wide range of wavelengths and it can be simultaneously utilized to generate multiple different colored QDs under a single wavelength.⁴³ The quantum mechanical model explains how the energy of an emitted photon is dependent upon the size of the region to which the energy is confined.⁴⁴ This means that the larger the QDs, the smaller the energy difference between the highest occupied molecular orbital (HOMO) and the lowest unoccupied molecular orbital (LUMO), and also lower is the energy of the emitted photon.⁴⁵ The surface carboxylic acids on some QDs can react with other functional groups such as primary amine groups on the N-terminus of the peptides by forming stable covalent bonds.⁴⁶ QDs have been used for rapid and precise quantitative determination of proteins/viruses by using its fluorescent intensity.⁴⁷ QDs have also been used for quantification of nucleic acid, single nucleotide polymorphism analysis as well as detection of aptamer-specific biomolecules.⁴⁸

5.3 Graphene oxides as biosensors

Graphene oxide (GO) two-dimensional nanosheet is a unique material produced by the oxidation of graphite.⁴⁹ A 2D structure of a GO sheet in figure 4 shows that various oxygen containing functional groups such as epoxides, carbonyl, carboxyl and hydroxyl groups are present on a monomolecular graphite.⁴⁹ High quality GO monolayers with excellent sheet-like properties have been synthesized by the mechanical exfoliation and chemical vapor deposition (CVD) methods.⁵⁰ GO can be used in a potential biosensor with strong quenching ability because of sp^2 hybridization, $\pi-\pi^*$ and $n-\pi^*$ interactions and various bioconjugation properties.⁵¹ GO can interact with DNA or other biomolecules through covalent, non-covalent or electrostatic interactions.⁵²

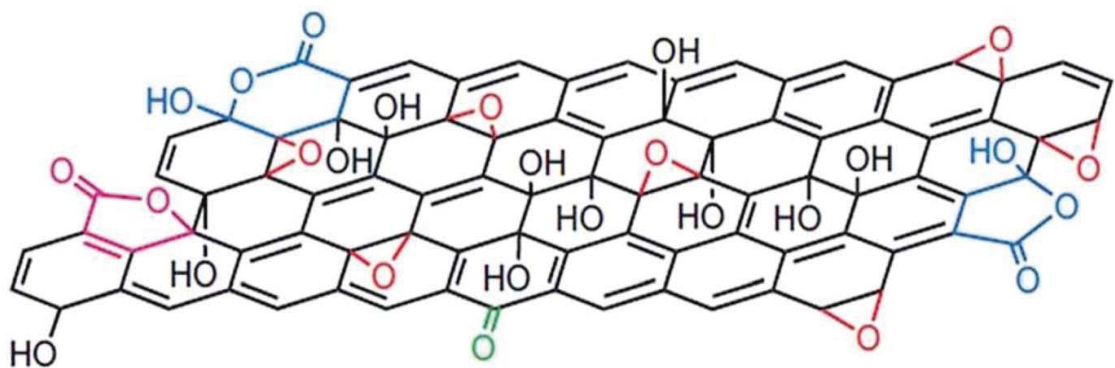


Figure 4. Structure of a monolayer graphene oxide showing various oxygen containing functional groups (Singh et. al, 2016)

6. Aims of Study

This study focuses on developing a non-PCR-based detection method using quantum dots (QDs) and graphene oxide (GO) in our signal transduction system. Our study is based

on hypothesis that QD-labeled TALEs can be adsorbed onto proximal GO sheets through hydrophobic interactions, π - π stacking interactions between the aromatic graphene rings and aromatic side chains available on the side chains of proteins, and some hydrogen bonds between hydrophilic side chains on the protein and hydrophilic groups on the edge of the GO sheets. These interactions are weak and reversible. A schematic diagram of our approach is represented in Figure 5. As QD-labeled TALEs are adsorbed on GO surface, the distance between the QD and GO gets closer and when QD emits a photon, it is absorbed and dispersed by GO. This causes overall decrease in QD signal, resulting in signal quenching via FRET. Since FRET can easily be broken by conformational changes, our approach utilizes this phenomenon upon target binding to the QDs-labeled TALEs, resulting in dissociation from the GO. When bound to target DNA, TALEs change into dense and short sunflower conformation and the interactions between TALEs and GO are weakened, leaving the GO surface. Thus, the distance between QDs and GO is becoming farther, which reduces a FRET effect, ultimately restoring QD signal. We will engineer TALEs to be able to recognize the *stx2* gene present in *E.coli* O157. Next, we will optimize the concentration of GO used in our assay and determine the sensitivity of our system.

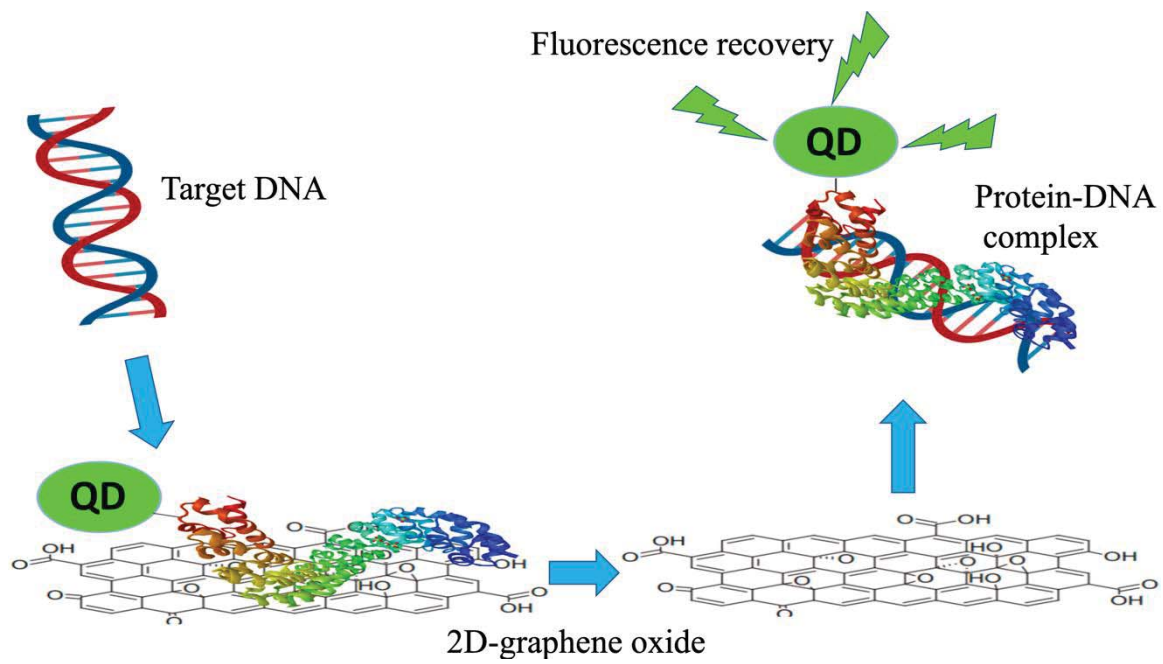


Figure 5. A schematic diagram showing GO-FRET based assay using QD-labeled TALEs for detecting dsDNA

CHAPTER II. EXPERIMENTAL

1. Engineering of TALEs

TALE proteins have N- and C-terminal truncated regions. TALE proteins were constructed to be specific to the DNA sequences of the *stx2* gene. TALE *stx_236* and *stx_255* were subcloned between *StuI* and *AatII* sites of the pMAL-c2X vector, replacing AvrBs3 TALE. The pMAL-c2X vector contains Maltose-Binding Protein (MBP) and Histidine (His) purification tag. Table 1 includes the TALE *stx2* 236 RVD sequences as well as their target nucleotides. A 17.5 repeat long DNA-binding region starting with a 5' thiamine was constructed by using four nucleotides specific RVDs that specifies a single DNA base, respectively. This repeat region recognizes 18 base pair (bp) long DNA sequences which is long enough to specify a unique single site in the *E. coli* genome.

Table 1. TALE *stx2* 236 RVD sequences and their target sequence in Shiga Toxin gene *stx2*

5'→3' DNA sequence (238-258)	G	A	T	G	T	C	T	A	T	C	A	G	G	C	G	C	G
TALE (A) <i>stx2</i> 236 RVDs	NN	NI	NG	NN	NG	HD	NG	NI	NG	HD	NI	NN	NN	HD	NN	HD	NN

2. Expression and purification of TALEs

The TALE expression and purification are completed in four days. On day 1, 10 inoculation tubes each containing 5 mL of culture were prepared. Each culture tube consists of 5 mL of Luria-Bertani (LB) medium, 2.5 µL of Ampicillin (Amp) and a single colony from a plate containing BL-21 *E. coli* transformed with *stx2* 236 TALE. The cultures were

grown overnight (16-18 hours) in a shaker incubator at 37°C and 250 rpm. On day 2, the culture tubes were removed from the shaker and kept at 4°C for additional 6 hours. 2 L of cell culture was made by adjusting the final volume of culture required to produce enough proteins. Two Erlenmeyer flasks each being able to hold at least twice the final volume were used. For each liter, 975 mL of LB media, 487.5 µL of Amp and five of 5 mL inoculations from day 1 were added. Then, the cells were incubated in a shaker incubator at 37°C and 250 rpm. The optical density (OD) of the cells were read at regular intervals using a UV-Vis spectrophotometer (Thermo Scientific) at 600 nm, keeping in mind that the cells grow exponentially with doubling time of about 20 minutes. When the OD reaches 0.4-0.5, the cultures were placed on ice and stirred occasionally until OD = 0.6. Then, the cells were induced with 0.1 mM Isopropyl β-D-1-thiogalactopyranoside (IPTG) at 250 rpm overnight at 16°C. On day 3, the culture from a flask is divided into six Beckmann tubes and centrifuged at 3500 rpm for 20 minutes. The procedure is repeated for another flask of culture. The pellets can be stored at -80°C upto 3 days. On day 4, the pellets were resuspended using 25 mL of Lysis buffer (2 mM Sodium Azide, 500 mM Sodium Chloride, 5 mM Imidazole, 20 mM Tris Cl, pH 7.9). The cells were then lysed using a sonicator on 50% amplitude, for 7, 10 second intervals with 20 seconds breaks in between and a final 10 sec sonication. The lysed cells were then centrifuged at 15,000 rpm for 40 minutes. The cell lysate was collected and purified using a Nickel (Ni) column (Thermo Fisher). In a cold room, a Ni-column of bed height 2-3 cm was prepared and allowed to set for 30-60 minutes. The column was equilibrated with 75 mL of Lysis buffer. The lysate was syringe-filtered and then passed through the column. The column was then washed with 100 mL of Lysis buffer, 100 mL of High Salt Wash buffer (2 mM Sodium Azide, 2 M Sodium

Chloride, 5 mM Imidazole, 20 mM Tris Cl pH 7.9) and finally 100 mL of Lysis buffer to remove unbound proteins. The protein was then eluted with 10 mL of Elution buffer (2 mM Sodium Azide, 500 mM Sodium Chloride, 500 mM Imidazole, 20 mM Tris Cl pH 7.9). The protein fractions were buffer exchanged with TALE storage buffer (480 mM Potassium Chloride, 1.6 mM Ethylene diammine tetra-acetic acid (EDTA), 25 mM Tris Cl pH 7.5) using a 10,000 Da filter (Pierce, Rockford, IL, USA) and stored in ice at 4°C until further use. The concentrations of proteins are determined by Bradford assay and the purity of proteins is known by running an SDS-page gel.

3. Preparation of GO

GO dispersion (ACS Material, Pasadena, CA, USA) is vortexed to ensure homogeneous solution before diluting using water. A serial dilution was performed for the preparation of different GO concentrations. The stock GO dispersion of 5 mg/mL is initially diluted to 1 mg/mL, and subsequently diluted to 20 µg/mL, with 100 µg/mL decrease in concentration from 1 mg/mL to 100 µg/mL, and 10 µg/mL decrease in concentration from 100 µg/mL to 20 µg/mL of GO. For TEM observation, the sample was prepared by depositing a droplet of GO dispersion on a lacey formvar films on copper TEM grid.

4. Quantum dot labeling

Using 1-Ethyl-3-(3-dimethylaminopropyl) carbodiimide (EDC) and N-Hydroxy succinimide (NHS) coupling, the Carboxy polyethylene glycol (PEG) functionalized CdSe/ZnS quantum dots in water having emission peak of 520 nm (Creative Diagnostics,

Shirley, NY, USA) were covalently conjugated with TALEs. The formation of a stable peptide bond is depicted in figure 6 using EDC/NHS bioconjugation. Free carboxyl groups react with EDC crosslinker to form an unstable o-Acylisourea intermediate. This intermediate on reaction with free amino groups can form a stable peptide bond or can react with Sulfo-NHS to give a Sulfo-NHS ester, which on further reaction with free amino groups gives a stable peptide linkage. For conjugation reaction, the molar ratio of QD:EDC:NHS was determined to be 1:4000:8000. For the labeling experiment, 10 μ L of 10 μ M QDs were added to 70 μ L of HEPES buffer (20 mM HEPES, 90 mM KCl, 1 mM MgCl₂ and 100 mM ZnCl₂ at pH 7.5). Then, 10 μ L of 40 mM EDC (Thermo Scientific, Rockford, IL, USA) and 10 μ L of 80 mM NHS (Thermo Scientific, Rockford, IL, USA) were added to the solution and mixed end-to-end using a Hula-mixer. After 20 minutes of mixing, 100 μ L of about 5 μ M TALEs was added and mixed end-to-end in the mixture for additional 2 hours. The mixture was then filtered for separating unlabeled TALEs and excess EDC/NHS in the flow-through, using 0.5 mL 100 K ultrafiltration unit (Pierce, Rockford, IL, USA) at 15,000 x g for 10 minutes. The concentration of unlabeled TALEs in the flow-through was calculated using Bradford assay. The concentration of unlabeled TALEs was subtracted from the initial concentration of TALEs to determine the concentration of the QD-labeled TALEs. The labeled protein was stored in TALE Storage Buffer (480 mM KCl, 1.6 mM EDTA, 2 mM DTT, 12 mM Tris-Cl, pH 7.5) in dark at 4°C until further use.

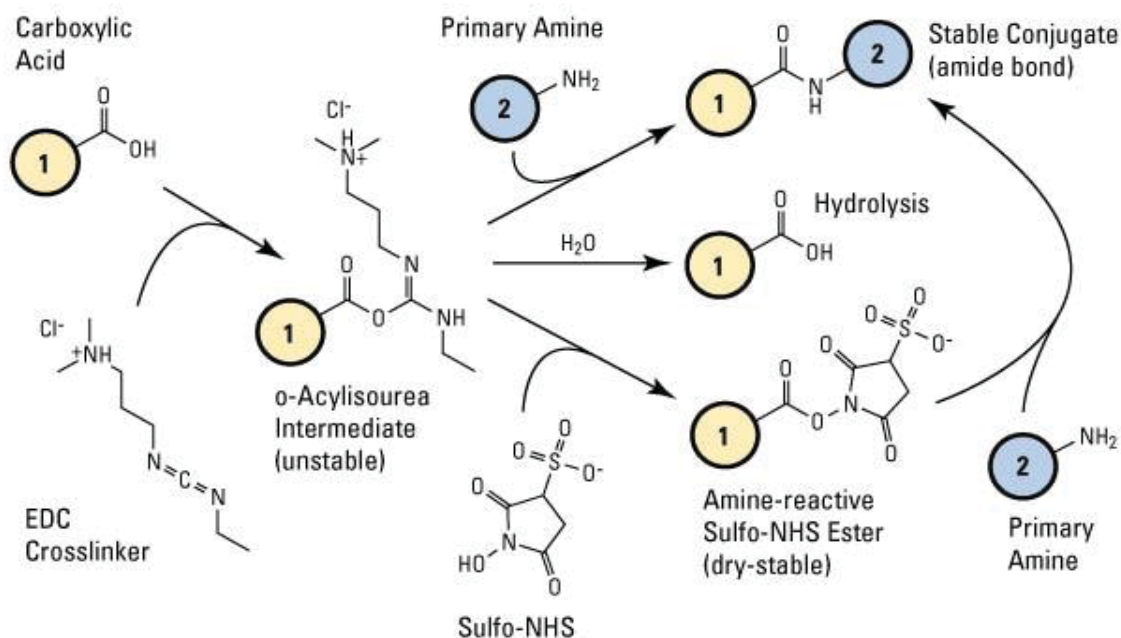


Figure 6. EDC/NHS bioconjugation chemistry showing the formation of a stable peptide bond (Thermo Fisher Scientific)

5. Graphene oxide quenching

Using several different concentrations of GO (ACS Material, Pasadena, CA, USA) and 10 nM of QD-labeled TALEs, a quenching assay was run to calculate the fluorescent quenching efficiency of the labeled protein by the GO. The stock GO dispersion of 5 mg/mL was diluted to 1 mg/mL and then serially to one-tenth in the final reaction concentration using deionized water. The concentration of GO used for the experiment ranges from 10 $\mu\text{g/mL}$ to 1000 $\mu\text{g/mL}$. Each experiment was run in duplicate using opaque black 96-well plates (Corning, Kennebunk, ME, USA). The final reaction volume was made up to 200 μL with PBS before mixing by pipetting and allowed it to incubate for 10 minutes in dark. Quenching was then measured by exciting the QDs using 370 nm light. Using Synergy H1 multi-plate reader (BioTek Instruments, Winooski, VT, USA), the

fluorescent spectral scanning was performed ranging from 400 nm to 600 nm with an interval of 5 nm and gain of 75 along with a final 515 nm endpoint fluorescence measurement. The fluorescent quenching efficiency was calculated for each experimental GO concentration in the range by dividing the observed fluorescence (F) to the maximum fluorescence at no GO (F₀) multiplied by 100% and then subtracting the obtained value from 100%.

$$\% \text{ Quenching efficiency} = 100 - \frac{F}{F_0} \times 100$$

6. TALE-GO assay

The TALE assay with GO was performed in an opaque black 96-well plate (Corning, Kennebunk, ME, USA). In each well, 20 μ L of GO dispersion, 20 μ L of QD-labeled TALEs, 20 μ L appropriate target DNA and finally 140 μ L of TALE Storage Buffer were added in duplicate to bring up a final volume of 200 μ L. Each sample was then mixed by pipetting and allowed to incubate at room temperature in dark for 10 minutes. Using Synergy H1 multi-plate reader (BioTek Instruments, Winooski, VT, USA), the fluorescence intensity was measured with excitation wavelength (λ_{ex}) of 370 nm and emission wavelength (λ_{em}) of 515 nm.

CHAPTER III. RESULTS AND DISCUSSION

1. Expression and purification of TALEs

TALE stx2-236 was expressed in BL-21 E. coli cells using IPTG induction. It required only a week to culture, express and isolate bacterial cells. A Bradford assay was run to determine the concentration of protein which resulted in 1 mL of 14.83 μ M of TALE protein. An SDS-PAGE gel was run to check the purity of the protein and the size of purified proteins. The gel image is shown in figure 7 where lane 1 represents a protein standard marker while lanes 2 through 8 represent samples. This result was consistent with the theoretical predicted protein size of 110.3 kDa due to the presence of full N and C terminus flanking regions as well as MBP used to increase the total protein solubility.

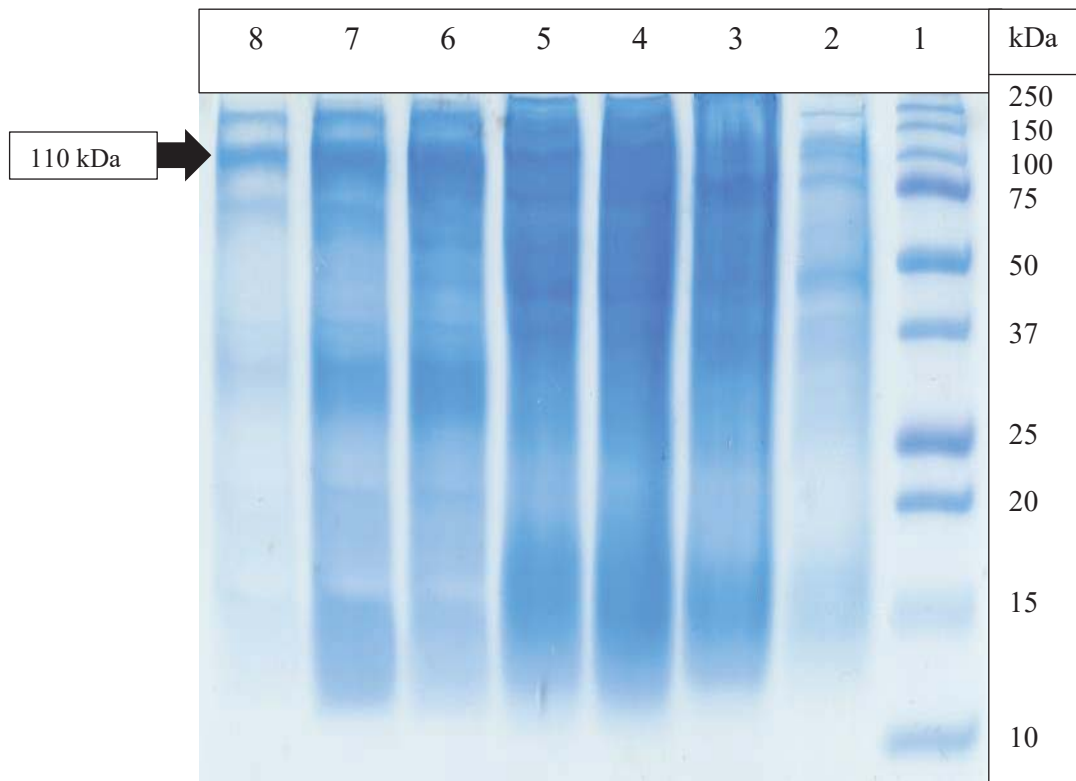


Figure 7. SDS-PAGE gel of TALE stx2 236 from *E. coli* BL-21 expression and purification. From the right, lane 1 contains a protein standard marker. Lanes 2 and 3 contain bacterial culture collected before and after IPTG induction respectively. Lane 4 contains lysate before passing through the Ni-column and Lane 5 is the flow-through. Lanes 6, 7 and 8 are the eluted protein fractions.

The bacterial expression system is very practical than other expression system because it is a long-term method of protein expression. Several glycerol stocks of the transformed BL-21 cells can be prepared and stored at -80 °C for several years which can be easily streaked onto a LB-agar-AMP plate. The colonies of bacterial cells can be used to prepare large volume culture of cells in a very short period of time. This method is so viable in research where only few proteins need to be produced before materials must be stored.

2. Characterization of GO

The single layer ratio was > 80% with the GO size ranging from 0.5 to 2 μm and width of 3 to 5 nm. The morphology of GO was measured using Transmission Electron Microscopy (TEM) JEM-1400plus (JOEL, Peabody, MA, USA). A TEM image showed that GO is indeed a monolayer with occasional folds and wrinkles (Fig 8). The size of bare GO ranged from 0.5 to 2 μm . The TEM image in Figure 9 showed that the size of QD-labeled TALEs was estimated to be in the range of several nanometers (5-7 nm) and QDs-labeled TALEs were adsorbed onto the GO surface. This supports our approach where the fluorescence of QDs labeled on TALEs would be quenched on the GO surface via FRET. The core diameter of QDs is approximately 6 nm. The diameter of a TALE protein can be calculated to be 5.6 nm using the following equation,

$$R_{min} = \left(\frac{3V}{4\pi}\right)^{\frac{1}{3}} = 0.066M^{\frac{1}{3}}$$

where, R_{min} is a radius of the protein in nanometer and M is the molecular mass of the protein in Dalton. The above equation is based on two assumptions; (i) the protein has spherical shape and (ii) the estimated size is equal to the minimal radius in the given mass of protein.

The height profile of bare GO is shown in Figure 10 (B), indicating the thickness of 4-5 nm. The approximate height of QD-labeled TALEs adsorbed on GO ranged from 11-17 nm which is indicated by the AFM image (Fig. 11 (B)). This AFM data supports the TEM data, confirming that QD-TALEs are indeed adsorbed on GO sheet.

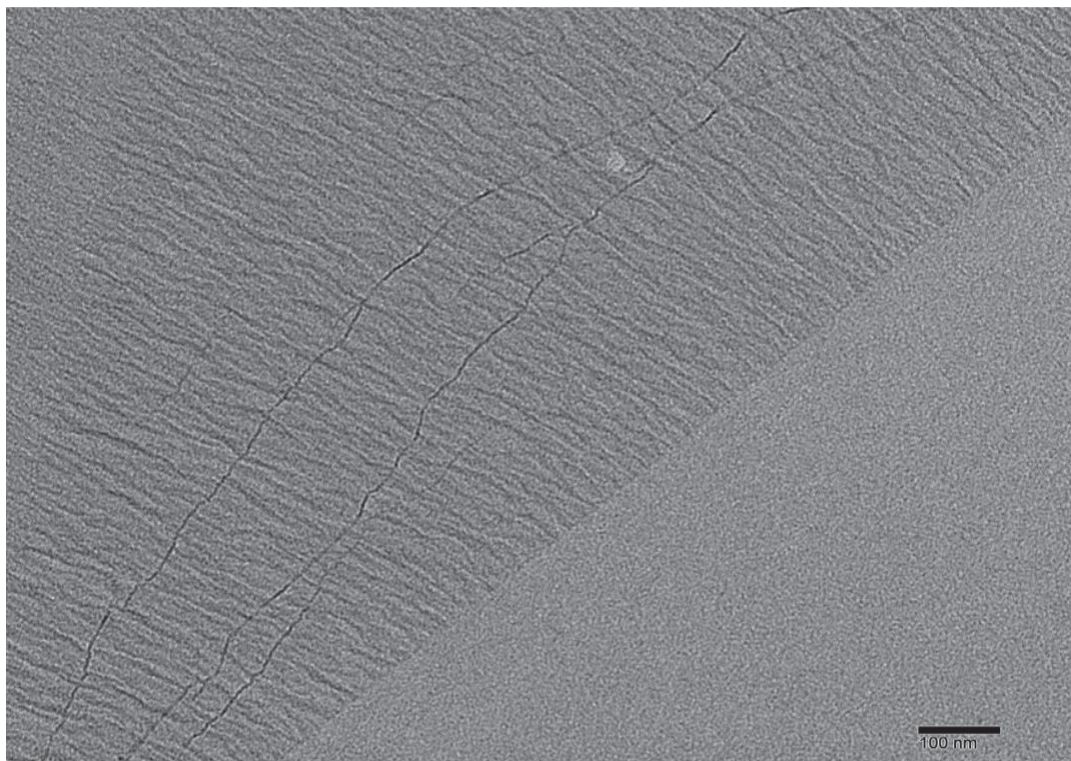


Figure 8. TEM image of monolayer GO sheets

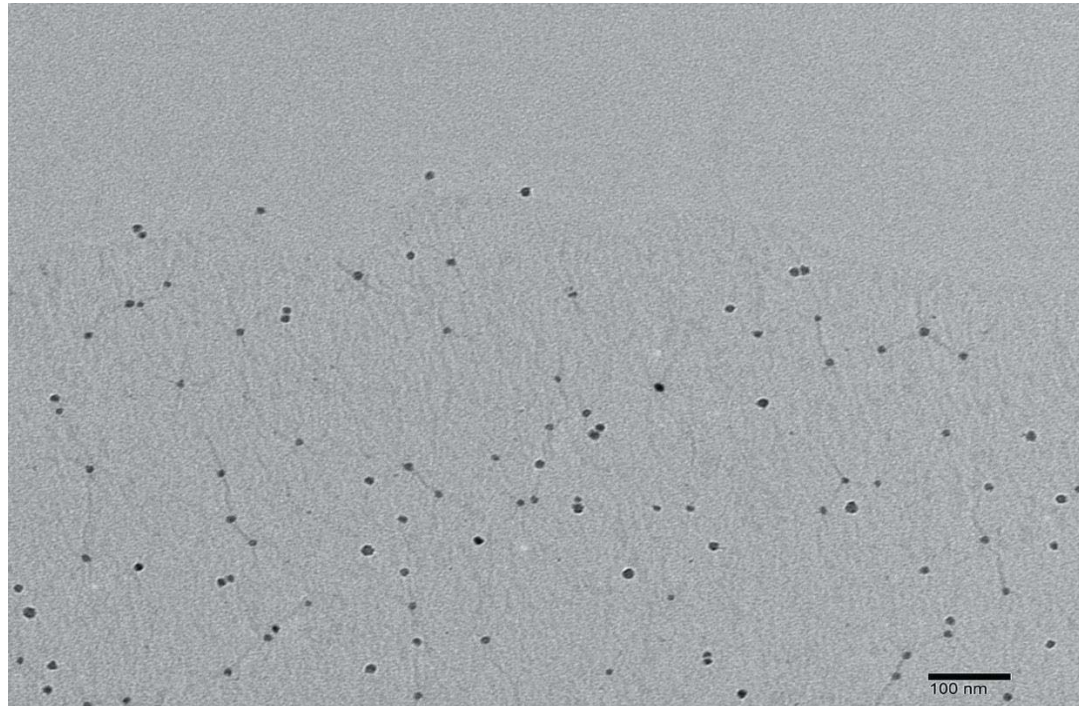


Figure 9. TEM image of QD-labeled stx2 236 TALEs on GO surface

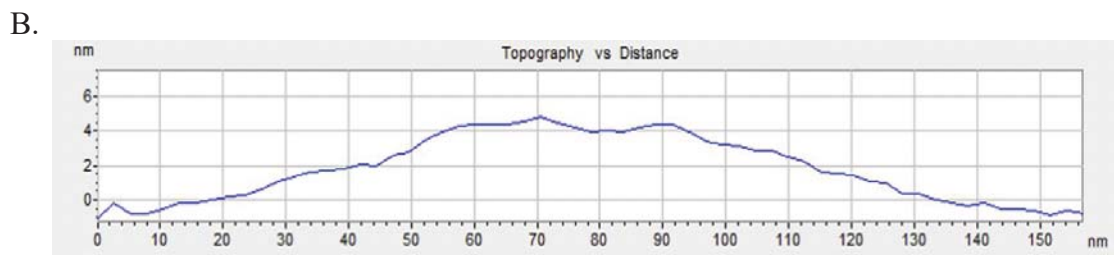
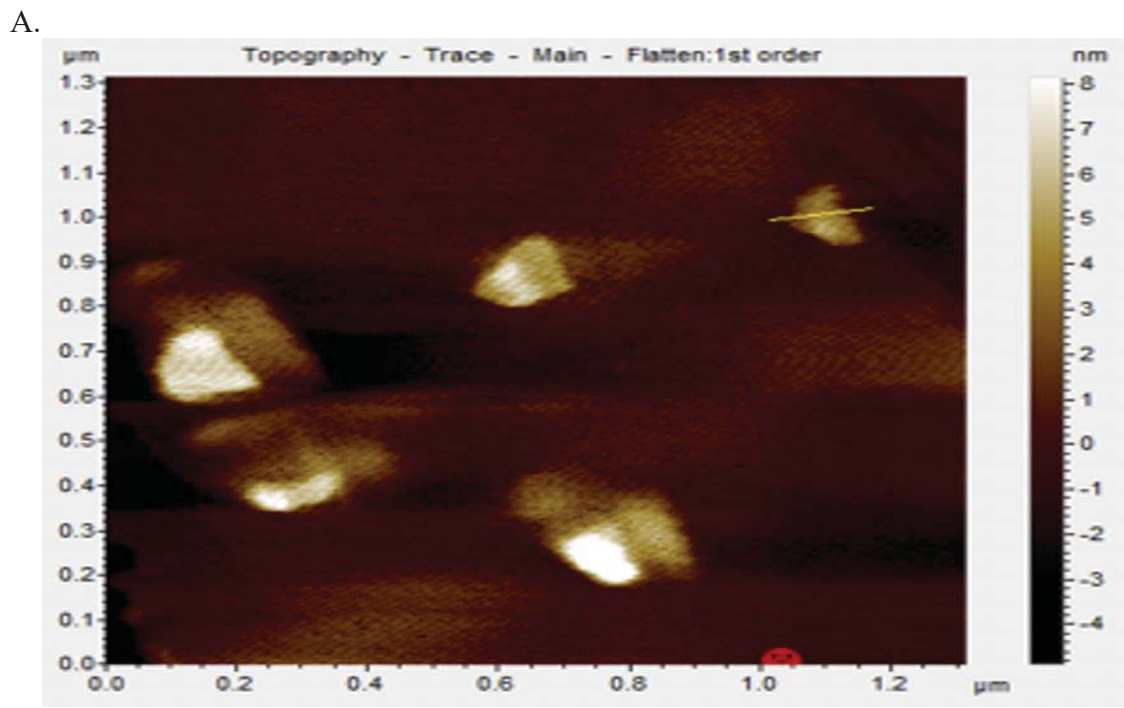
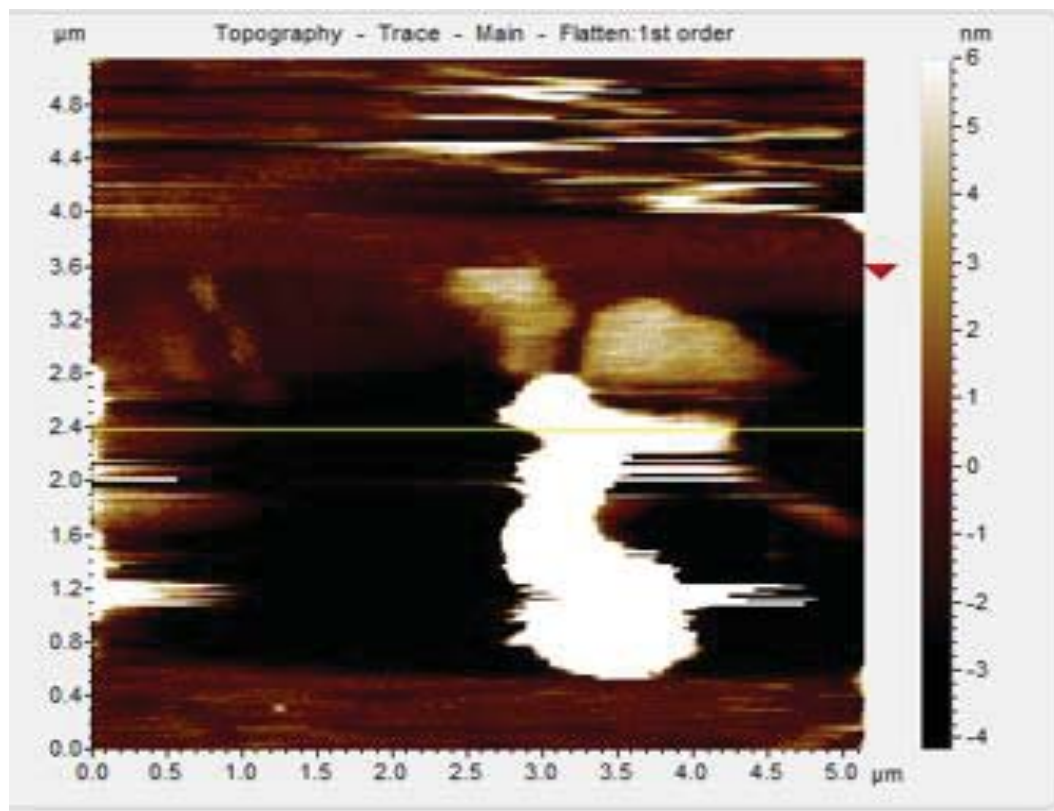


Figure 10. (A) AFM image of QD-labeled stx2 236 TALEs on GO surface and (B) the height profile of the corresponding yellow line

A.



B.

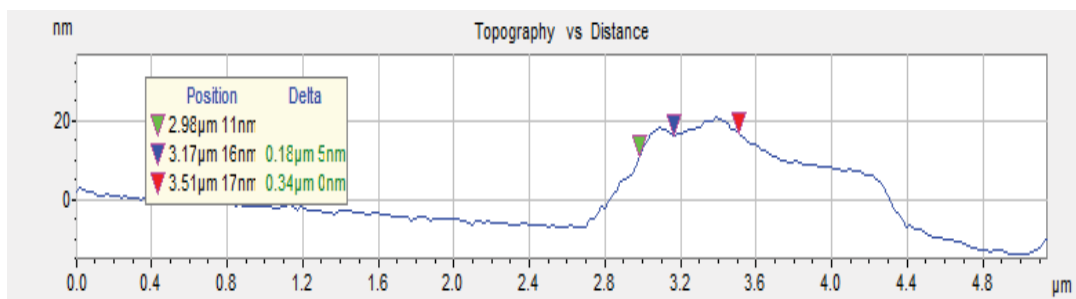


Figure 11. (A) AFM image of QD-labeled stx2 236 TALEs on GO surface and (B) the height profile of the corresponding yellow line

3. Quantum dot labeling of TALEs

The concentration of proteins before labeling was 6.4 μM and the final concentration of QD-labeled proteins was 6.31 μM , which indicates a labeling efficiency of 98.5%. This data was significantly better than the previous values obtained on TALE labeling efficiency as well as the values obtained for Zinc Finger Proteins (ZFPs) in our lab using the same method. The labeled TALE protein is stable and can be used for up to two weeks because the total fluorescence rapidly decreases after two weeks.

4. GO Quenching Efficiency

The quenching of the QD-labeled TALEs was completed within one week to minimize system errors. A quenching array was completed to determine the lowest concentration of GO in the stable and linear region determined experimentally. Beyond this region, the relative fluorescence becomes unpredictable, which may be because of oversaturation of GO. When GO becomes oversaturated, the dissociation of QD-labeled TALEs from GO would not create enough distance between the QDs and the GO. This would cause a system error due to the significant amounts of background FRET. This has been observed in previous experiments with ZFPs and GO in the Kim Lab at WKU.

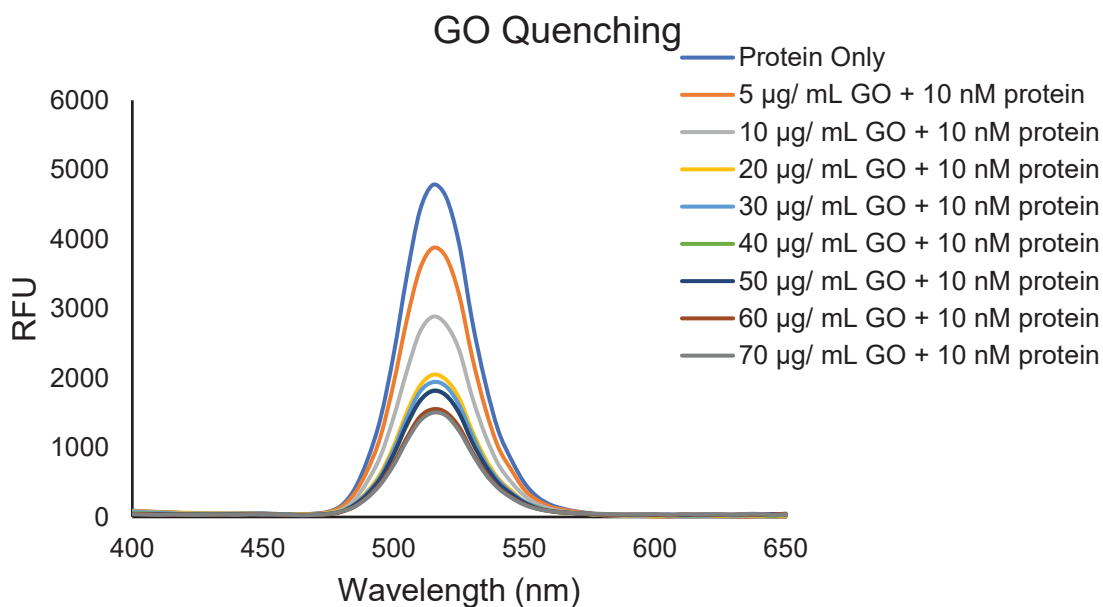
GO is known as a universal quencher of fluorescence for molecules such as peptides/proteins, quantum dots and organic dyes. The quenching effect of GO concentration on QD-labeled TALEs was investigated over a range of 0 to 70 $\mu\text{g/mL}$ as shown in Figure 12. A Stern-Volmer plot of F_0/F was plotted as a function of the concentration GO where F_0 and F were the fluorescence intensity at the maxima in the absence and presence of GO, respectively as shown in Figure 12 (B). This plot shows a

linear quenching effect of GO when GO was added to the solution containing the QD-labeled protein. The quenching efficiency of QD-labeled TALEs by GO was calculated using the following equation where F_0 and F were the fluorescence intensity at the maxima in the absence and presence of GO, respectively.

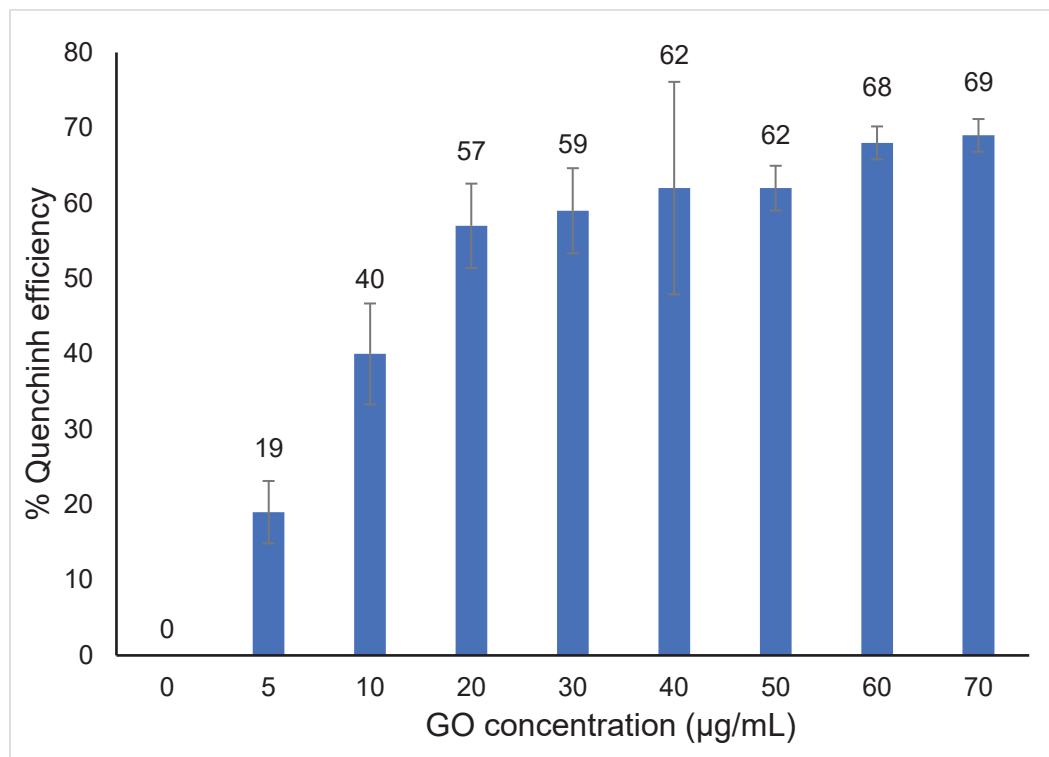
$$\% \text{ Quenching efficiency} = 100 - \frac{F}{F_0} \times 100$$

The GO concentration range was examined in duplicate for both endpoint and spectrum quenching data. It was determined that 10 nM protein concentration was sufficient for quenching assay. At the concentration of 10 $\mu\text{g}/\text{mL}$ of GO, there was a rapid decrease in fluorescence intensity of the QD-labeled TALEs with a quenching efficiency of about 40%. A linear trend in increasing quenching efficiency was observed with increasing GO concentration.

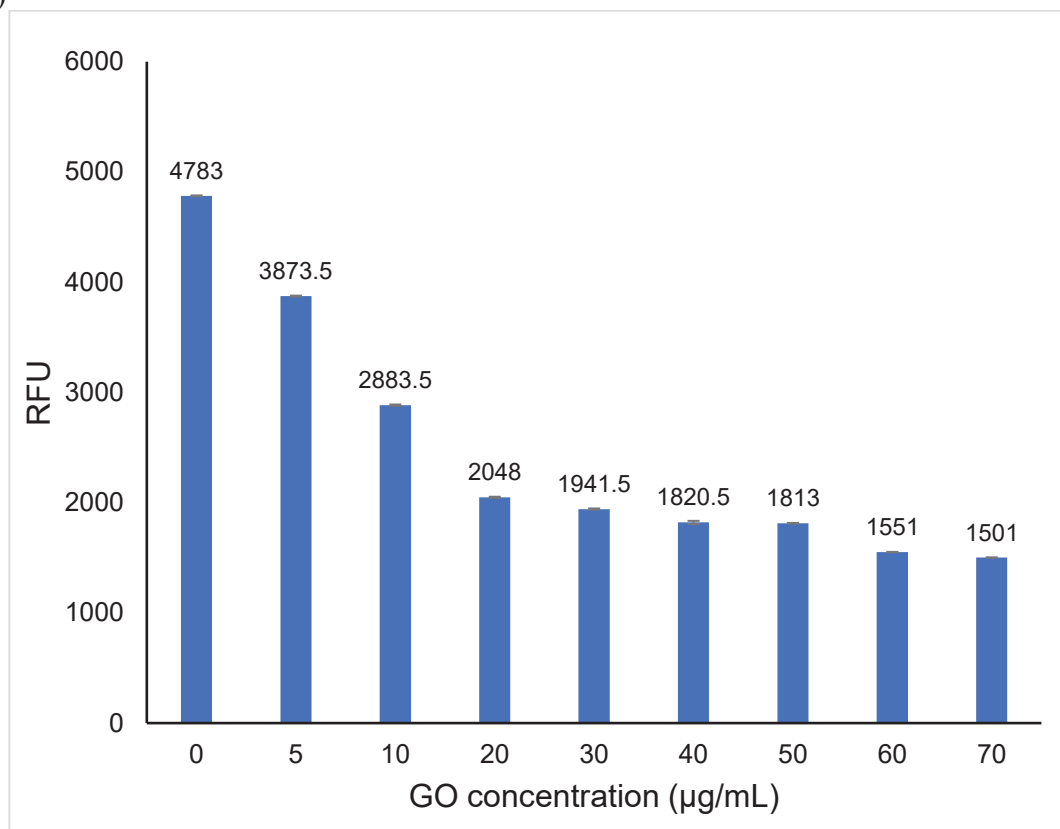
(A)



(B)



(C)



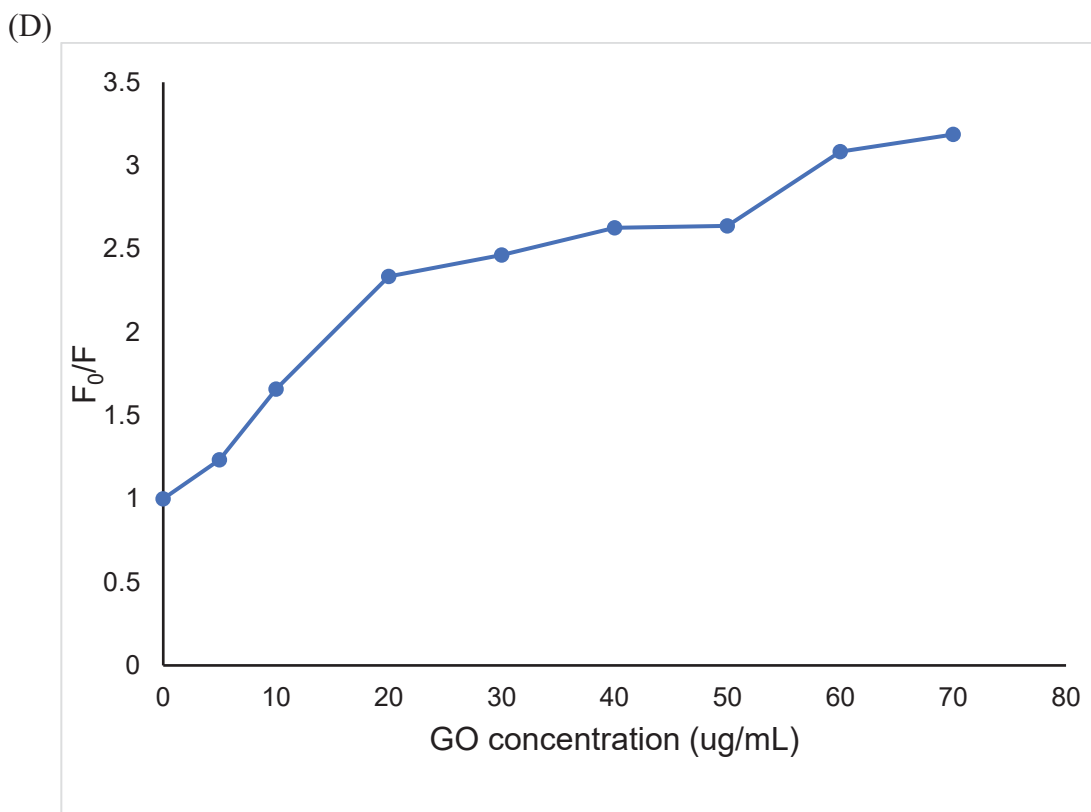


Figure 12. (A) Changes in fluorescence spectra, (B) quenching efficiency, (C) fluorescence intensity of QDs-labeled TALEs with increasing concentrations of GO from 0 to 70 ug/mL, (D) Stern-Volmer plot of QD-labeled TALEs versus increasing concentration of GO.

We have found from the previous studies in the Kim Lab that excess GO might be unfavorable for the sensing system due to desorption of TALEs from GO surface. Thus, we believe that using the minimum amount of GO for the assay would better distinguish signals from varying DNA concentrations. We ran a fluorescence quenching assay to determine the fluorescence quenching efficiency of the QD-labeled TALEs by GO, at GO concentrations less than 10 $\mu\text{g/mL}$ (Fig 13). At the concentration of 10 $\mu\text{g/mL}$ of GO, the fluorescence quenching efficiency was calculated to be 47%, which was consistent with

the previous report of 40% for the same concentration of GO. At 2 $\mu\text{g}/\text{mL}$ of GO, a fluorescence quenching efficiency of 10% was calculated. For GO concentration less than 2 $\mu\text{g}/\text{mL}$, there was hardly any quenching, which could be because of incomplete adsorption of GO of TALEs on GO surface. Therefore, 2 $\mu\text{g}/\text{mL}$ of GO was used preliminarily for the assay.

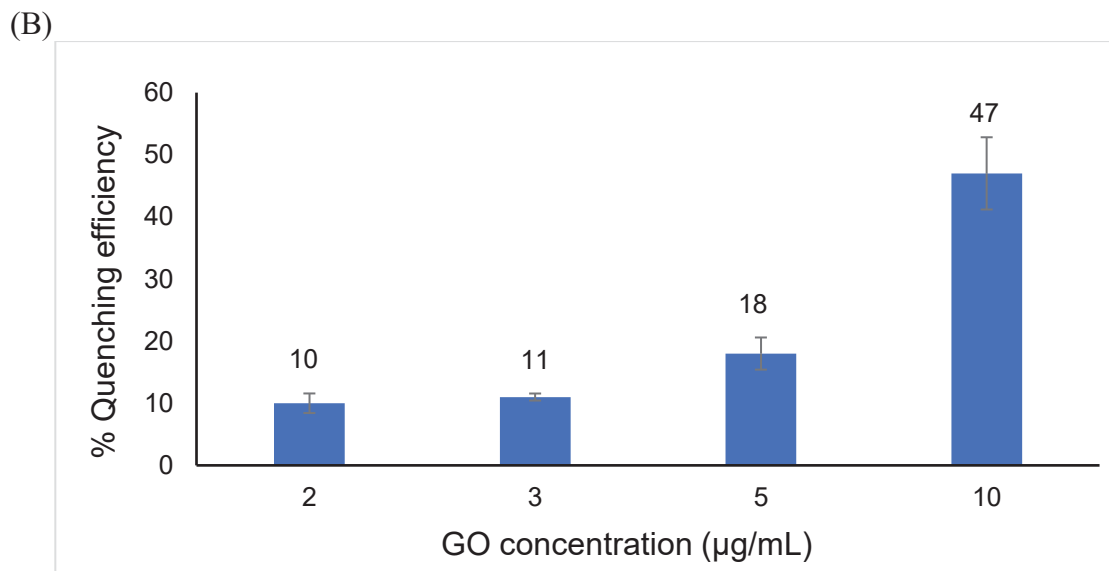
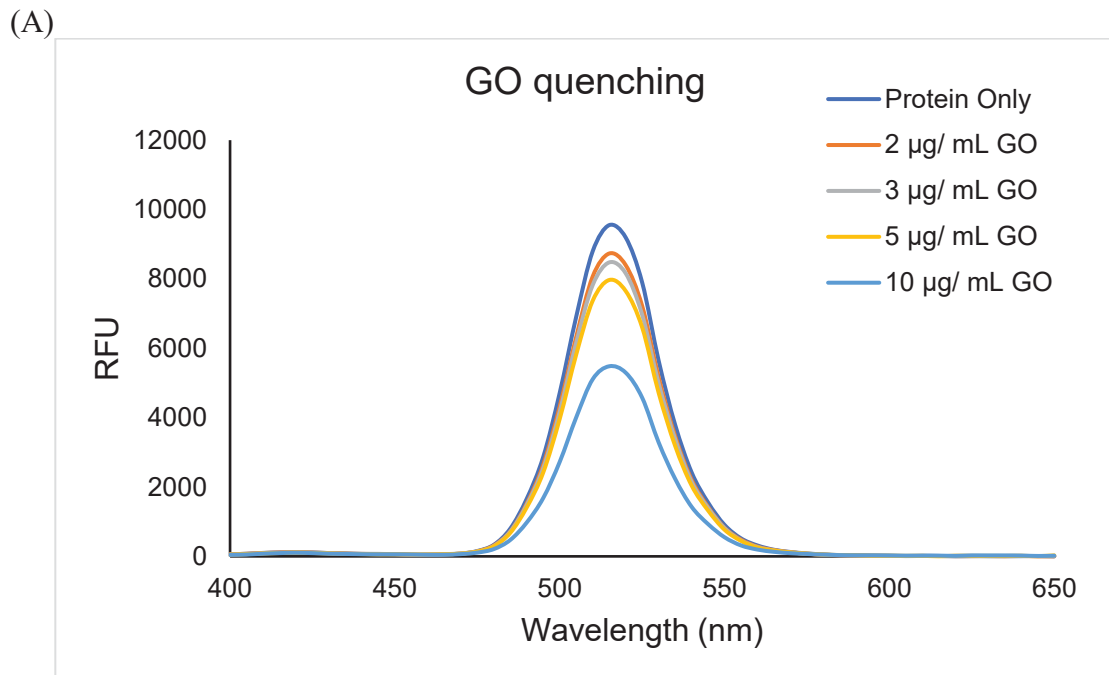


Figure 13. Fluorescence spectral change (A) and fluorescence quenching efficiency (B) due to increasing concentration of GO from 0 to 10 $\mu\text{g/mL}$.

5. Sensitivity

To determine the sensitivity of our system, we performed TALE assay at various concentrations of target stx2-236 DNA ranging from 50 nM to 1 nM. The percentage fluorescence recovery was calculated using the following equation where F_0 and F were the fluorescence intensity at the maxima in the absence and presence of GO, respectively and F_i was the fluorescence intensity at the maxima in the presence of target DNA.

$$\% \text{ Fluorescence recovery} = 100 - \frac{F_0 - F_i}{F_0 - F_1} \times 100$$

At the concentration of 1nM DNA, a fluorescence recovery of 30% was obtained, which was consistent with the previously obtained values for ZFP stx2 268 (Fig 14). We also believe that a lower limit of detection could potentially be achieved. Two different concentrations of DNA at 0.2 nM (200 pM) and 0.5 nM (500 pM) were examined. There was a linear increase in fluorescence recovery with increase in the DNA concentration. The limit of detection of target stx2 236 TALE was determined to be 200 pM, which is equal to 40 fmol of target oligonucleotides.

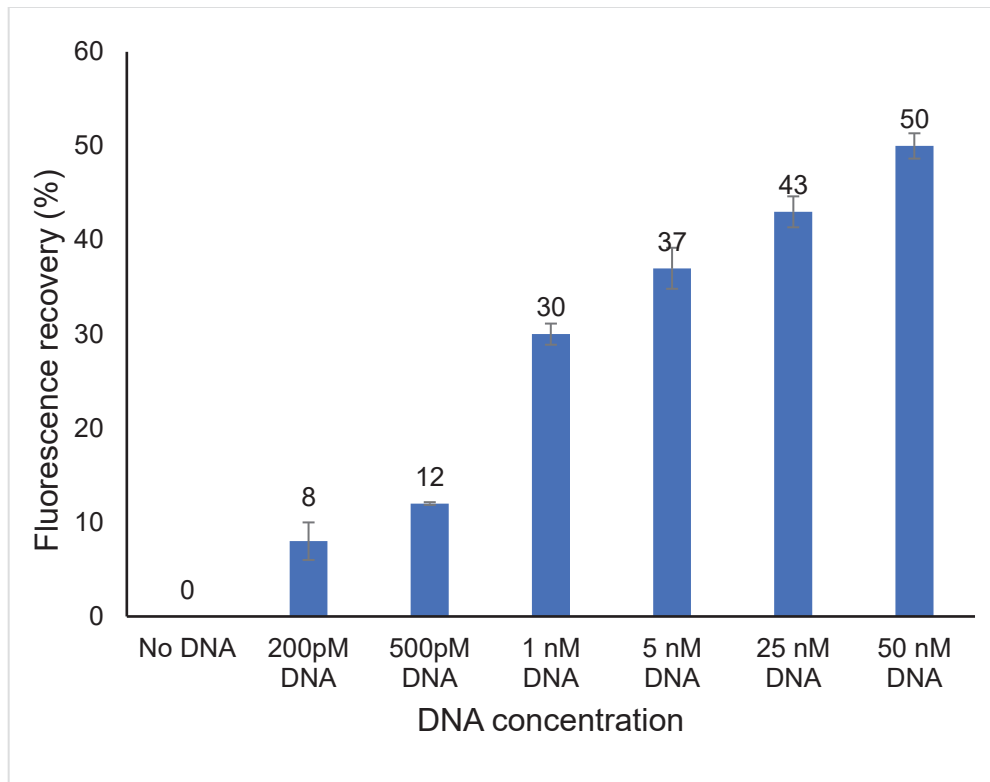


Figure 14. The limit of detection of TALE stx2 236

CHAPTER IV. CONCLUSION

In this study, TALEs were designed to recognize the *stx2* gene present in pathogenic *E. coli* and we were able to express and purify TALEs using Ni-NTA resin. The *E. coli* BL-21 expression system is quicker than plant expression system requiring only a week to culture, express and isolate the bacterial cells. The labeling of TALEs with QDs using EDC and NHS bioconjugation resulted in >90% labeling efficiency. This data was significantly better than the previous values obtained in TALE labeling efficiency as well as the values obtained for Zinc Finger Proteins (ZFPs). This novel sensing system avoids requiring of multiple laborious steps in DNA denaturation and subsequent hybridization and also does not require the labeling of DNA. The TEM and AFM results supported our approach where the fluorescence of QDs labeled with TALEs would be quenched on the GO surface via FRET. The fluorescence of QDs was quenched by GO linearly before the system becomes saturated with GO. The fluorescence signal was restored when the target DNA bound to TALE proteins. TALE proteins show high sensitivity towards their own target DNA, allowing for developing a novel and reliable method of pathogen detection. TALE proteins showed the best sensitivity at 20 nM of labeled TALEs and 3 µg/mL of GO. Adding 40 mM MgCl₂ and 2 mM DTT in the assay buffer seems to improve the sensitivity of the labeled TALE for its target DNA. Our GO-based sensor along with TALEs provided a detection limit of 200 pM of the target *stx2* gene. In conclusion, we successfully demonstrated the novel application of a new class of DNA-binding protein TALEs and 2D nanosheet GO for pathogen detection.

As a next step, we will investigate our system with another protein TALE stx2 255 and newly designed TALEs that recognize the antibiotic resistance gene, for example, the *tetM* gene (tetracycline resistance gene). We will examine the sensitivity of the labeled TALE proteins in the presence of genomic DNA because this system did not quantify background signal, which could occur in the presence of multiple non-target DNA. Further studies will examine the system's applicability to sensitively and specifically detect the crude biological samples such as cell lysates in order to validate our system for the use of a rapid and reliable method for detecting pathogenic bacteria at real world settings.

BIBLIOGRAPHY

1. Huang, J.; Su, X.; Li, Z., Enzyme-Free and Amplified Fluorescence DNA Detection Using Bimolecular Beacons. *Analytical chemistry (Washington)* **2012**, *84* (14), 5939-5943.
2. Wheeler, E. K.; Benett, W.; Stratton, P.; Richards, J.; Chen, A.; Christian, A.; Ness, K. D.; Ortega, J.; Li, L. G.; Weisgraber, T. H.; Goodson, K.; Milanovich, F., Convectively Driven Polymerase Chain Reaction Thermal Cycler. *Analytical chemistry (Washington)* **2004**, *76* (14), 4011-4016.
3. Liu, R. H.; Yang, J.; Lenigk, R.; Bonanno, J.; Grodzinski, P., Self-Contained, Fully Integrated Biochip for Sample Preparation, Polymerase Chain Reaction Amplification, and DNA Microarray Detection. *Analytical chemistry (Washington)* **2004**, *76* (7), 1824-1831.
4. Tjong, V.; Yu, H.; Hucknall, A.; Rangarajan, S.; Chilkoti, A., Amplified On-Chip Fluorescence Detection of DNA Hybridization by Surface-Initiated Enzymatic Polymerization. *Analytical chemistry (Washington)* **2011**, *83* (13), 5153-5159.
5. Yu, C.-Y.; Yin, B.-C.; Wang, S.; Xu, Z.; Ye, B.-C., Improved Ligation-Mediated PCR Method Coupled with T7 RNA Polymerase for Sensitive DNA Detection. *Analytical chemistry (Washington)* **2014**, *86* (15), 7214-7218.
6. Kim, B. C.; Park, J. H.; Gu, M. B., Multiple and Simultaneous Detection of Specific Bacteria in Enriched Bacterial Communities Using a DNA Microarray Chip with Randomly Generated Genomic DNA Probes. *Analytical chemistry (Washington)* **2005**, *77* (8), 2311-2317.

7. de Lambert, B.; Chaix, C.; Charreyrex, M.-T.; Laurent, A.; Aigoui, A.; Perrin-Rubens, A.; Pichot, C., Polymer–Oligonucleotide Conjugate Synthesis from an Amphiphilic Block Copolymer. Applications to DNA Detection on Microarray. *Bioconjugate chemistry* **2005**, *16* (2), 265-274.
8. Peterson, E. M.; Manhart, M. W.; Harris, J. M., Competitive Assays of Label-Free DNA Hybridization with Single-Molecule Fluorescence Imaging Detection. *Analytical chemistry (Washington)* **2016**, *88* (12), 6410-6417.
9. Ha, D. T.; Ghosh, S.; Ahn, C. H.; Segal, D. J.; Kim, M.-S., Pathogen-specific DNA sensing with engineered zinc finger proteins immobilized on a polymer chip. *Analyst (London)* **2018**, *143* (17), 4009-4016.
10. Kim, M.-S.; Kim, J., Multiplexed detection of pathogen-specific DNA using engineered zinc finger proteins without target amplification. *Analytical methods* **2016**, *8* (37), 6696-6700.
11. Kim, M.-S.; Kini, A. G., Engineering and Application of Zinc Finger Proteins and TALEs for Biomedical Research. *Molecules and cells* **2017**, *40* (8), 533-541.
12. Honarmand, A.; Mayall, R.; George, I.; Oberding, L.; Dastidar, H.; Fegan, J.; Chaudhuri, S.; Dole, J.; Feng, S.; Hoang, D.; Moges, R.; Osgood, J.; Remondini, T.; van der Meulen, W. K.; Wang, S.; Wintersinger, C.; Zapparoli Zucoloto, A.; Chatfield-Reed, K.; Arcellana-Panlilio, M.; Nygren, A., A Multiplexed Transcription Activator-like Effector System for Detecting Specific DNA Sequences. *ACS synthetic biology* **2014**, *3* (12), 953-955.

13. Imanishi, M.; Matsumura, K.; Tsuji, S.; Nakaya, T.; Negi, S.; Futaki, S.; Sugiura, Y., Zn(II) Binding and DNA Binding Properties of Ligand-Substituted CXHH-Type Zinc Finger Proteins. *Biochemistry (Easton)* **2012**, *51* (16), 3342-3348.
14. Ooi, A. T.; Stains, C. I.; Ghosh, I.; Segal, D. J., Sequence-Enabled Reassembly of β -Lactamase (SEER-LAC): A Sensitive Method for the Detection of Double-Stranded DNA. *Biochemistry (Easton)* **2006**, *45* (11), 3620-3625.
15. Boch, J.; Bonas, U., Xanthomonas AvrBs3 Family-Type III Effectors: Discovery and Function. *Annual review of phytopathology* **2010**, *48* (1), 419-436.
16. Mak, A. N. S.; Bradley, P.; Bogdanove, A. J.; Stoddard, B. L., TAL effectors: function, structure, engineering and applications. *Current Opinion in Structural Biology* **2013**, *23* (1), 93-99.
17. Zhang, M. J.; Wang, F.; Li, S. F.; Wang, Y.; Bai, Y.; Xu, X. Q., TALE: A tale of genome editing. *Progress in Biophysics & Molecular Biology* **2014**, *114* (1), 25-32.
18. Erkes, A.; Reschke, M.; Boch, J.; Grau, J., Evolution of Transcription Activator-Like Effectors in *Xanthomonas oryzae*. *Genome biology and evolution* **2017**, *9* (6), 1599-1615.
19. Meckler, J. F.; Bhakta, M. S.; Kim, M.-S.; Ovadia, R.; Habrian, C. H.; Zykovich, A.; Yu, A.; Lockwood, S. H.; Morbitzer, R.; Elsässer, J.; Lahaye, T.; Segal, D. J.; Baldwin, E. P., Quantitative analysis of TALE–DNA interactions suggests polarity effects. *Nucleic acids research* **2013**, *41* (7), 4118-4128.
20. Tsuji, S.; Imanishi, M., Modified nucleobase-specific gene regulation using engineered transcription activator-like effectors. *Advanced Drug Delivery Reviews* **2019**, *147*, 59-65.

21. Cuculis, L.; Abil, Z.; Zhao, H.; Schroeder, C. M., Direct observation of TALE protein dynamics reveals a two-state search mechanism. *Nature communications* **2015**, *6* (1), 7277.
22. Morbitzer, R.; Elsaesser, J.; Hausner, J.; Lahaye, T., Assembly of custom TALE-type DNA binding domains by modular cloning. *Nucleic acids research* **2011**, *39* (13), 5790-5799.
23. Scott, J. N. F.; Kupinski, A. P.; Boyes, J., Targeted genome regulation and modification using transcription activator-like effectors. *The FEBS journal* **2014**, *281* (20), 4583-4597.
24. Cermak, T.; Doyle, E. L.; Christian, M.; Wang, L.; Zhang, Y.; Schmidt, C.; Baller, J. A.; Somia, N. V.; Bogdanove, A. J.; Voytas, D. F., Efficient design and assembly of custom TALEN and other TAL effector-based constructs for DNA targeting. *Nucleic acids research* **2011**, *39* (17), 7879-7879.
25. Hu, Johnny H.; Davis, Kevin M.; Liu, David R., Chemical Biology Approaches to Genome Editing: Understanding, Controlling, and Delivering Programmable Nucleases. *Cell chemical biology* **2016**, *23* (1), 57-73.
26. Mussolino, C.; Morbitzer, R.; Lütge, F.; Dannemann, N.; Lahaye, T.; Cathomen, T., A novel TALE nuclease scaffold enables high genome editing activity in combination with low toxicity. *Nucleic acids research* **2011**, *39* (21), 9283-9293.
27. Sun, N.; Liang, J.; Abil, Z.; Zhao, H. M., Optimized TAL effector nucleases (TALENs) for use in treatment of sickle cell disease. *Molecular Biosystems* **2012**, *8* (4), 1255-1263.

28. Ousterout, D. G.; Perez-Pinera, P.; Thakore, P. I.; Kabadi, A. M.; Brown, M. T.; Qin, X.; Fedrigo, O.; Mouly, V.; Tremblay, J. P.; Gersbach, C. A., Reading Frame Correction by Targeted Genome Editing Restores Dystrophin Expression in Cells From Duchenne Muscular Dystrophy Patients. *Molecular therapy* **2013**, *21* (9), 1718-1726.
29. Mahfouz, M. M.; Li, L.; Piatek, M.; Fang, X.; Mansour, H.; Bangarusamy, D. K.; Zhu, J.-K., Targeted transcriptional repression using a chimeric TALE-SRDX repressor protein. *Plant molecular biology* **2011**, *78* (3), 311-321.
30. Zhang, Q.; Robin, K.; Liao, D.; Lambert, G.; Austin, R. H., The Goldilocks Principle and Antibiotic Resistance in Bacteria. *Molecular pharmaceutics* **2011**, *8* (6), 2063-2068.
31. Xu, J.-G.; Cheng, B.-K.; Jing, H.-Q., Escherichia Coli O157 H7 and Shiga-like-toxin- producing Escherichia Coli in China. *World journal of gastroenterology : WJG* **1999**, *5* (3), 191-194.
32. Schüller, S., Shiga Toxin Interaction with Human Intestinal Epithelium. *Toxins* **2011**, *3* (6), 626-639.
33. Beceiro, A.; Tomas, M.; Bou, G., Antimicrobial Resistance and Virulence: a Successful or Deleterious Association in the Bacterial World? *Clinical microbiology reviews* **2013**, *26* (2), 185-230.
34. Fakruddin, M.; Mannan, K. B.; Hossain, M.; Islam, S.; Mazumdar, R.; Chowdhury, A.; Chowdhury, M., Nucleic acid amplification: Alternative methods of polymerase chain reaction. *Journal of pharmacy & bioallied science* **2013**, *5* (4), 245-252.

35. Sekar, R. B.; Periasamy, A., Fluorescence resonance energy transfer (FRET) microscopy imaging of live cell protein localizations. *The Journal of cell biology* **2003**, *160* (5), 629-633.
36. Bajar, B.; Wang, E.; Zhang, S.; Lin, M.; Chu, J., A Guide to Fluorescent Protein FRET Pairs. *Sensors (Basel, Switzerland)* **2016**, *16* (9), 1488.
37. Bunt, G.; Wouters, F. S., FRET from single to multiplexed signaling events. *Biophysical reviews* **2017**, *9* (2), 119-129.
38. Birch, D. J. S.; Rolinski, O. J., Fluorescence resonance energy transfer sensors. *Research on Chemical Intermediates* **2001**, *27* (4-5), 425-446.
39. Matea, C.; Mocan, T.; Tabaran, F.; Pop, T.; Mosteanu, O.; Puia, C.; Iancu, C.; Mocan, L., Quantum dots in imaging, drug delivery and sensor applications. *International journal of nanomedicine* **2017**, *12*, 5421-5431.
40. Yue, Z.; Lisdat, F.; Parak, W. J.; Hickey, S. G.; Tu, L.; Sabir, N.; Dorfs, D.; Bigall, N. C., Quantum-Dot-Based Photoelectrochemical Sensors for Chemical and Biological Detection. *ACS applied materials & interfaces* **2013**, *5* (8), 2800-2814.
41. Pleskova, S.; Mikheeva, E.; Gornostaeva, E., Using of Quantum Dots in Biology and Medicine. In *Cellular and Molecular Toxicology of Nanoparticles*, Saquib, Q.; Faisal, M.; AlKhedhairi, A. A.; Alatar, A. A., Eds. Springer International Publishing Ag: Cham, 2018; Vol. 1048, pp 323-334.
42. Jha, S.; Mathur, P.; Ramteke, S.; Jain, N. K., Pharmaceutical potential of quantum dots. *Artificial Cells, Nanomedicine, and Biotechnology: Supplement 1* **2018**, *46* (sup1), 57-65.

43. Mo, D.; Hu, L.; Zeng, G.; Chen, G.; Wan, J.; Yu, Z.; Huang, Z.; He, K.; Zhang, C.; Cheng, M., Cadmium-containing quantum dots: properties, applications, and toxicity. *Applied microbiology and biotechnology* **2017**, *101* (7), 2713-2733.
44. Kawaguchi, K.; Ito, H.; Kuwahara, T.; Higuchi, Y.; Ozawa, N.; Kubo, M., Atomistic Mechanisms of Chemical Mechanical Polishing of a Cu Surface in Aqueous H₂O₂: Tight-Binding Quantum Chemical Molecular Dynamics Simulations. *ACS applied materials & interfaces* **2016**, *8* (18), 11830-11841.
45. Cooper, W. F.; Clark, G. A.; Hare, C. R., A simple, quantitative molecular orbital theory. *Journal of chemical education* **1971**, *48* (4), 247.
46. Jin, S.; Hu, Y.; Gu, Z.; Liu, L.; Wu, H.-C., Application of Quantum Dots in Biological Imaging. *Journal of nanomaterials* **2011**, *2011*, 1-13.
47. Chen, L.; Zhang, X.; Zhou, G.; Xiang, X.; Ji, X.; Zheng, Z.; He, Z.; Wang, H., Simultaneous Determination of Human Enterovirus 71 and Coxsackievirus B3 by Dual-Color Quantum Dots and Homogeneous Immunoassay. *Analytical chemistry (Washington)* **2012**, *84* (7), 3200-3207.
48. Dong, H.; Gao, W.; Yan, F.; Ji, H.; Ju, H., Fluorescence Resonance Energy Transfer between Quantum Dots and Graphene Oxide for Sensing Biomolecules. *Analytical chemistry (Washington)* **2010**, *82* (13), 5511-5517.
49. Chiu, N.-F.; Huang, T.-Y.; Lai, H.-C.; Liu, K.-C., Graphene oxide-based SPR biosensor chip for immunoassay applications. *Nanoscale research letters* **2014**, *9* (1), 1-7.
50. Thangamuthu, M.; Hsieh, K. Y.; Kumar, P. V.; Chen, G.-Y., Graphene- and Graphene Oxide-Based Nanocomposite Platforms for Electrochemical Biosensing Applications. *International journal of molecular sciences* **2019**, *20* (12), 2975.

51. Balaji, A.; Yang, S.; Wang, J.; Zhang, J., Graphene Oxide-Based Nanostructured DNA Sensor. *Biosensors (Basel)* **2019**, *9* (2), 74.
52. Lee, J.; Kim, J.; Kim, S.; Min, D. H., Biosensors based on graphene oxide and its biomedical application. *Advanced Drug Delivery Reviews* **2016**, *105*, 275-287.